# Non-Invasive Continuous Real-Time Blood Glucose Estimation Using PPG Features-based Convolutional Autoencoder with TinyML Implementation

Noor Faris Ali, Alyazia Aldhaheri, Bethel Wodajo, Meera Alshamsi, Shaikha Alshamsi, Mohamed Atef

Electrical and Communications Engineering Department, United Arab Emirates University, 15551, Al Ain, United Arab Emirates

2024 IEEE International Symposium on Circuits and Systems (ISCAS) | 979-8-3503-3099-1/24/$31.00 ©2024 IEEE | DOI: 10.1109/ISCAS58744.2024.10558453

***Abstract*— In this paper, we developed a convolutional autoencoder for non-invasive continuous monitoring of blood glucose levels (BGL) using four photoplethysmography (PPG) features. The model was specifically designed to account for temporal relations among consecutive PPG segments' features and transient outliers encountered in real-time operation. By means of Tiny Machine Learning (TinyML), the model was embedded in an edge device, Arduino Nano 33 BLE Sense, for real-time continuous predictions of BGL. On a PC, the model was tested using a public dataset of 33 subjects and achieved a mean absolute error (MAE) 5.55 mg/dL, standard error of prediction (SEP) 7.18 mg/dL, and 97.57% success rate in zone A of Clarke error grid (CEG). On the edge, the model was tested on new 8 subjects and obtained a MAE 5.16 mg/dL and 100% of predicted BGL falling into zone A. Overall, the integration of the proposed model and the feature set resulted in substantial gains in terms of applicability, effectiveness, efficiency, and interpretability on both cloud and edge infrastructures.**

***Keywords – Blood Glucose, PPG, Machine Learning, Convolutional Autoencoder, TinyML, MCU***

## I. INTRODUCTION

Diabetes is a worldwide prevalent health issue [1]. It is a chronic illness characterized by abnormal blood glucose levels (BGL) due to either insulin resistance or pancreas malfunction [2]. Long-term hyperglycemia results in adverse effects on the heart, eyes, kidneys, and nerves [3-4]. Therefore, it is vital to monitor BGL regularly and continuously to identify diabetes progressive patterns and ensure early diagnosis to avoid improper or delayed treatment and organs dysfunction [2].

A photoplethysmography (PPG) signal integrated with machine learning is currently being investigated to remedy the shortcomings of current invasive BGL monitoring devices [3-4].

In the study presented in [5], a hardware PPG system is proposed, and 4-min PPG signals were collected from 26 subjects for BGL estimation using an extreme gradient boost (XGB) model. Features including power spectral density (PSD), energy, spectral analysis, autoregressive coefficients, heart rate, breathing rate, BMI, and wavelet analysis were extracted.

Corresponding author: Mohamed Atef, Email: moh_atef@uaeu.ac.ae

This research was funded by the United Arab Emirates University, Arab Emirates, under Grant G00004481 and partially funded by G00004546.

The work in [6] has introduced Mel frequency cepstral coefficients (MFCC) features of PPG signal along with age, weight, and height as input for XGB.

Reference [7] has proposed the combination of dual-wavelength PPG and bioelectrical impedance for BGL estimation. Data was collected from 40 subjects. Features such as mean, variance, skewness, kurtosis, standard deviation, and information entropy were calculated from the PPG. Age, height, weight, heart rate, blood flow rate, hemoglobin, and pulse oximetry were also added as features to their backpropagation neural network (BPNN) model.

In another study [8], fingertip videos were collected from 93 subjects using a smartphone camera and lighting source. 21 features were selected from PPG, its derivatives, and Fourier transform (FFT). They included age and gender as well. The features were then fed to a deep neural network (DNN).

The work in [9] proposed a convolutional neural network (CNN) model that takes PPG signal along with the PSD mean as input. Additionally, they introduced a prototype consisting of a PPG sensor connected to Arduino Nano 33 BLE Sense for deployment.

In study [10], PPG signals were collected from 30 subjects and glucose levels were measured before and 2 hours after breakfast. The authors proposed a CNN model to automatically extract features from the PPG signal for BGL estimation.

The main gap in the literature is the limited research on model deployment in resource-constrained edge devices like MCUs to perform on-device real-time continuous BGL predictions. This is crucial as models' performance may deteriorate significantly when tested on the edge compared to cloud or server infrastructure. The core reason for this is the heterogeneity of both infrastructures. Edge devices are inherently restricted by memory and energy resources.

In this paper, we propose a convolutional autoencoder model that seeks to achieve balance between efficiency, interpretability, and accuracy. The proposed model takes PPG sequential segments features as input instead of raw PPG signals. Four features were extracted based on domain knowledge between PPG and BGL. The selected features require simple calculations to avoid computational burden of spectral analysis and data dimensionality of excessive features. The model is then deployed in an edge device, Arduino Nano Sense BLE 33, by means of Tiny Machine Learning (TinyML) and tested in real-time environment for continuous non-invasive predictions of BGL.

## II. METHODOLOGY

The methodological framework in this study involves two main branches, as depicted in Fig. 1. First, the model development stage, where we created and tested our model for BGL estimation on a cloud infrastructure, using a database. Second, TinyML implementation where we embedded our model in edge device and evaluated its performance on new subjects by acquiring PPG and running the application program and the deployed model in real-time environment.

### A. Database

We utilized a public database consisting of PPG signals derived from smartphone camera alongside the reference BGL measured invasively [11]. The database contains 197 trials for 52 subjects. After conducting a data anomaly and quality examination based on the clarity and appearance of vital PPG characteristics (systolic peaks and valleys), corrupted data were eliminated, and we ended up having data for 33 subjects. The blood glucose values range between 68 to 211 mg/dL.

### B. Signal Processing

To alleviate interfered noise with PPG, we harnessed a Butterworth 2nd order digital low-pass filter (LPF) designed with a cut-off frequency of 4 Hz to suppress undesired high-frequency noise. Moreover, a baseline wander removal method was employed by subtracting the signal average to remove DC offset. The amplitude of the PPG signal was normalized to a predefined range (from 0 to 1) using min-max formula. Each PPG segment represents a cardiac cycle containing two valleys and one systolic peak. Peaks and valleys were detected using adaptive thresholding and comparison of neighboring samples techniques.

### C. Feature Extraction

The features were selected based on the current domain knowledge about hemodynamic changes and vascular effects in response to BGL variations. According to the literature, several cardiovascular responses in cardiac output, blood volume, heart rate, and systematic vascular resistance can potentially occur due to changes in BGL [12]. A study [13] compared the PPG morphological distinctions at three BGL classes through statistical approaches. Remarkable relationships were identified between BGL and peak amplitude, position, and half-width. On this basis, we have selected four PPG features: Systolic amplitude (SA), heart rate (HR), peak width at half systolic amplitude (PW), and peak-to-valley interval or diastolic time (PVI), as shown in Fig. 2. With this selection, we are covering most of the relevant information needed for BGL estimation from PPG. SA has a strong correlation with cardiac output and vascular tone [14-15]. PW is correlated with vascular resistance [16]. HR is related to cardiovascular and autonomic nervous system responses to BGL changes [17]. PVI is representative of diastolic phase, which is slightly prolonged in healthy subjects compared to diabetic patients [17]. The main benefits of this compact feature set are calculations efficiency and interpretability. This approach significantly facilities human interpretation and model decision-making reasoning.

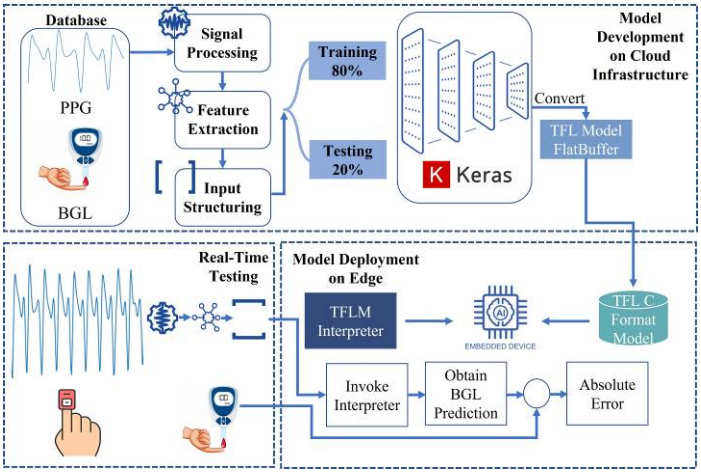


Fig.1. Methodological Framework: Model Development on Cloud and Deployment on Edge for Real-Time Testing.

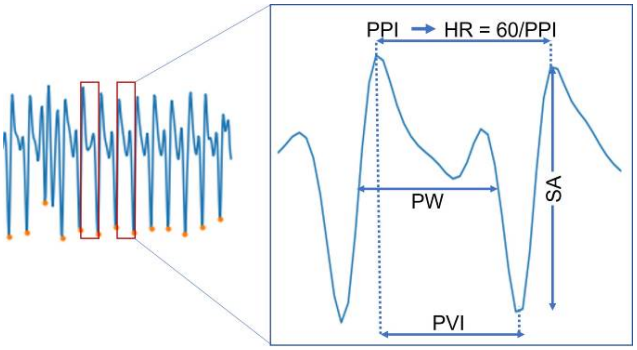


Fig. 2. Extracted PPG Features.

### D. Models Development and Training

The proposed model is inspired by convolutional autoencoder (CAE) topology. Classical CAE is used to filter noise in the input and create robust and stable feature representation through its bottleneck [18].

Instead of feeding the model with raw PPG signals, a 2D matrix consisting of eight sequential segments and the corresponding four extracted features is utilized as input to the model. As illustrated in Fig. 3, the model consists of three submodules: encoder, decoder, and a regression output layer. The model splits in a mirrored version of these layers, mimicking an autoencoder.

The input matrix enters two successive convolutional layers with kernels 4 and 2 and filters 32 and 16, respectively, and gets convolved with the kernels to extract abstracted features maps at different levels. Then, Average Pooling with a pool size of 2 is employed being the bottleneck of the autoencoder. To complete the autoencoder architecture, the decoder side is represented by a third convolutional layer followed by an up-sampling layer that accepts the compacted high-level features representation and reconstructs the activation map. It increases the dimensionality of the pooled feature maps, i.e., mapping the spatial dimensions of the third convolutional layer back into the same of the first convolutional layer.

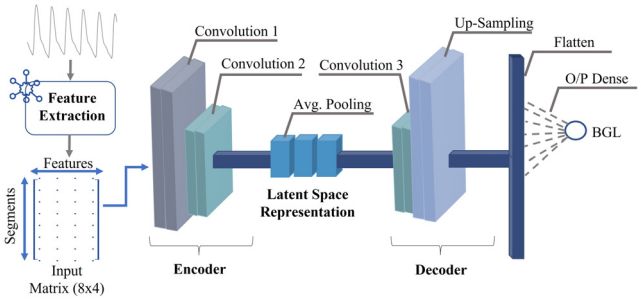


Fig.3. Proposed Model Architecture.

The up-sampling layer carries the fine-grained details of feature maps generated by the last convolutional layer, preserving representative features. Finally, a flattened layer followed by an output dense layer with Rectifier Linear Unit (ReLU) activation function assigned to perform the prediction of BGL.

In this manner, the model can 1) exploit the long-term temporal relations among successive segments' features, 2) capture richer representations, underlying complexities, and internal patterns within features, 3) filter redundant information and spot and mitigate outliers from the input segments through its bottleneck, and 4) obtain detailed and high-level features from the decoder module.

Experimental simulations validated the proposed model's efficiency and performance. The model's total internal parameters are 11,857 (46.32 KB). The proposed model delivered a MAE 5.55 mg/dL and SEP 7.18 mg/dL. The Clarke error grid (CEG) analysis showed that 97.57% of tested samples were in zone A and the rest were in zone B, which is clinically acceptable, see Fig.5 (a).

## III. RESULTS AND DISCUSSIONS

To test our developed model for real-time inference, we selected the Arduino Nano 33 BLE Sense MCU. It offers running edge computing applications using TinyML. It has a 1 MB Flash Memory and 256 KB SRAM and runs operations with a clock speed of 64 MHZ [19]. The proposed model built using Keras API was converted to Tensorflow Lite (TFL) FlatBuffer format. Then, the model was converted to a C byte array with hex representation using xxd command. The generated header file is then stored in Arduino's read-only program memory. The model is then interpreted by TensorFlow Lite for Microcontrollers (TFLM) API [20].

In the Arduino sketch, we declared pointers to the model, error reporter, input tensor, output tensor, and interpreter. Following, we created an operator resolver object that pulls in essential operations for the model implementation. Next, we declared tensor arena array. Finally, we created an interpreter instance.

As shown in Fig. 4, to obtain a BGL prediction, a streamlined raw input from a PPG sensor was recorded. The application code retrieves pointers to the memory regions that represent input tensor and fills them with the features values derived from the PPG signal (eight segments and corresponding four extracted features). Then, we invoke the interpreter to perform model calculations. The prediction is then accessed through

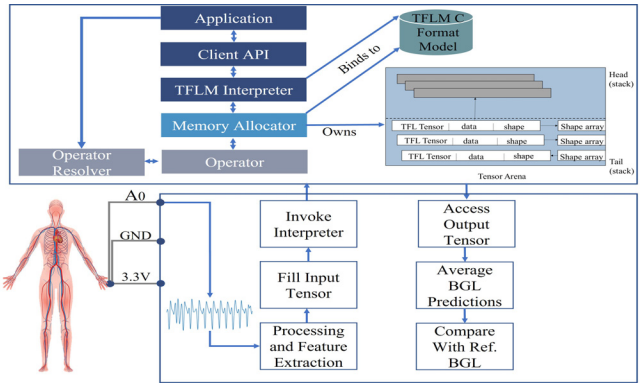


Fig.4. TinyML Implementation for Model Deployment in MCU.

the output tensor. We averaged eight consecutive BGL predictions, aiming for consistent behavior.

The proposed model was tested for its performance on new subjects in real-time. Eight subjects were recruited for real time measurements. The following steps were accomplished to test the model on each subject:

1. Reference BGL was measured using Accu–Chek glucometer.
2. The PPG sensor was attached to the subject's finger.
3. The TinyML-based program deployed on the Arduino IDE.
4. The features matrix (8*4) was passed to the input tensor.
5. Real-time BGL predictions were recorded and averaged.
6. The golden reference BGL was used to calculate the MAE.

TABLE I demonstrates the reference BGL measured and the average of the obtained eight consecutive BGL predictions by the embedded model. The results of the experiments found clear support for the effectiveness of the proposed model in real-time operation. Overall, the model achieved a MAE of 5.161 mg/dL. In addition, CEG analysis revealed that all the real-time BGL predictions by the deployed model lie within zone A with a success rate of 100%, See Fig.5 (b).

Looking at TABLE I, it is apparently seen that the model yielded superior performance on normal BGL cases. However, continuous BGL predictions for hyperglycemia cases (subjects #1 and #7) were slightly variable (higher MAE of 8 predictions). The model manifested better certainty and confidence in normal BGL cases. Nonetheless, we believe that the trend in our results is well justified by the limited observations of high BGL values in the training database. It is necessary to train the model on more hyperglycemia cases for better generalizability and confidence.

TABLE I Real-Time Testing Results of Deployed Model on MCU.

| Subject | Reference BGL (mg/dL) | On-Edge Average BGL (mg/dL) | MAE (mg/dL) |
|---|---|---|---|
| #1 | 149 | 151.27 | 9.76 |
| #2 | 96 | 99.95 | 4.98 |
| #3 | 107 | 107.51 | 4.96 |
| #4 | 94 | 94.67 | 3.37 |
| #5 | 127 | 125.45 | 2.27 |
| #6 | 117 | 115.95 | 1.17 |
| #7 | 183 | 179.72 | 10.02 |
| #8 | 111 | 109.02 | 4.74 |
| | | **Average MAE** | **5.16** |

Still, in all cases, predicted BGL values were within zone A of the CEG for real-time predictions and 97.57% for tested samples on PC, as shown in Fig. 5(a).

The undertaken empirical analysis implies that simulation results on the database (MAE 5.55) and real-time testing on edge (MAE 5.16) tie well with each other and were consistent. From this standpoint, it is sufficient to point out that the incorporation of the CAE and the selected four features yielded noteworthy results owing to the CAE capabilities of filtering noise and capturing temporal relations among segments, as well as the powerfulness of the minimal feature set.

TABLE II presents a comparison between the results of our proposed method with those of the previous studies. Our model outperforms the following models: PLS [11], XGB [5], and CNN [9]. From these results, we can show that our approach stands out with remarkable performance while retaining interpretability and efficiency and offering a TinyML-based solution for real-time predictions.

Considering the reported results, it is conceivable that handcrafted features-based models provide spectacular performance. For instance, XGB proposed by [6] used MFCC features and resulted in MAE of 1.76 mg/dL. A DNN model introduced in [8] was trained on 21 selected features including time-domain and frequency-domain features and achieved MAE of 5.4 mg/dL. The work in [7] proposed dual-wavelength PPG and bioelectrical impedance with frequency and statistical features as input to a BPNN. The model yielded MAE 5.0896 mg/dL.

Other studies have driven further development through multimodal approaches such as the fusion of ECG and PPG. In [21], authors have proposed a combination of dual-channel PPG amplitude features and ratios, and pulse arrival velocity from ECG and PPG using linear regression (LR). Overall, their model obtained a success rate of 100% in zone A. In study [22], authors introduced weight-based Choquet integral multimodal fusion for coupling different BGL monitoring algorithms based on the temporal statistical and spatial morphological features from ECG and PPG. Data was collected from 21 subjects. The model achieved 80.09% in zone A. Despite the satisfactory performance of most of these models, their applicability and practicability on edge have not been addressed sufficiently.

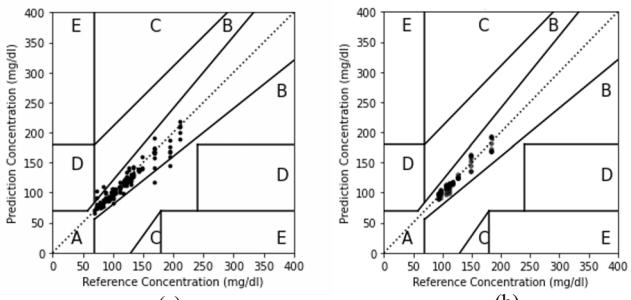


(a) (b)

Fig. 5. CEG Analysis of the proposed model on (a) PC using public dataset of 33 subjects, and (b) Edge with real-time operation on 8 subjects.

In edge infrastructure, efficiency is of critical importance. Thus, the computational burden associated with spectral analysis, excessive number of feature calculations, heavy architectures, and input multimodalities may not well-suit TinyML implementation. The restrictions of tiny devices may confine successful fitting and maintained long-term performance of models on MCU.

Compared to prior studies, our proposed model is interpretable, efficient, accurate, and deployable in TinyML-enabled resource-constrained edge devices. Our deployed handcrafted feature-based CAE model requires 279.85 KB (out of 1 MB Arduino's flash memory), including the model in TFL C format and all the processing and feature extraction operations done. In comparison, the CNN model developed for automated feature extraction by [9] required 700 KB. The extraction of only four features requiring simple calculations boosts efficiency drastically and avoids extended computational time and power and memory drainage. From an interpretability perspective, using evidence-based features physiologically associated with BGL makes our model more interpretable than relying on raw PPG or features having an ambiguous relationship with BGL.

TABLE II. Comparison with State-of-Art Models.

| Study | Subject | Range (mg/dL) | Model | MAE (mg/dL) | SEP (mg/dL) | Clarke Zone A% |
|---|---|---|---|---|---|---|
| [11] | 52 | 68-211 | PLS | - | 17.02 | - |
| [5] | 26 | 84-199 | XGB | 8.31 | - | 96.15 % |
| [6] | 217 | 58.6-390.7 | XGB | 1.76 | 5.53 | 98.97 % |
| [7] | 40 | 110 ± 15 | BPNN | 5.08 | - | 100% |
| [8] | 93 | - | DNN | 5.4 | - | - |
| [9] | 52 | 68-211 | CNN | 17.26 | - | 92.85 % |
| [21] | 18 | 75-180 | LR | RMSE= 7.46 | SD = 2.43 | 100% |
| Our Work (PC) | 33 | 68-211 | CAE | 5.55 | 7.18 | 97.57 % |
| Our Work (Edge) | 8 | 94-183 | CAE | 5.16 | 4.15 | 100% |

## IV. CONCLUSION

In this study, we proposed a model adopted from convolutional autoencoder topology. The model learns richer temporal representations and alleviates outliers' effects among PPG sequential segments' features to achieve better robustness and stability in real-time environment. The model was embedded in a MCU using TinyML and tested on new subjects. Our model resulted in outstanding performance on both cloud and edge infrastructures. The results point out the advantages and practicability of the proposed model and the minimal interpretable feature set for portable standalone PPG-based BGL monitoring.

## REFERENCES


[1] World Health Organization, “Diabetes,” World Health Organisation, Apr. 05, 2023. https://www.who.int/news-room/fact-sheets/detail/diabetes

[2] T. Zhu, K. Li, P. Herrero, and P. Georgiou, “Deep Learning for Diabetes: A Systematic Review,” IEEE Journal of Biomedical and Health Informatics, vol. 25, no. 7, pp. 2744–2757, Jul. 2021.

[3] W. Villena Gonzales, A. Mobashsher, and A. Abbosh, “The Progress of Glucose Monitoring—A Review of Invasive to Minimally and Non-Invasive Techniques, Devices and Sensors,” Sensors, vol. 19, no. 4, p. 800, Feb. 2019.

[4] E. Susana and K. Ramli, "Review of Non-Invasive Blood Glucose Level Estimation based on Photoplethysmography and Artificial Intelligent Technology," 2021 17th International Conference on Quality in Research (QIR): International Symposium on Electrical and Computer Engineering, Depok, Indonesia, 2021, pp. 158-163.

[5] S. Sen Gupta, T.-H. Kwon, S. Hossain, and K.-D. Kim, “Towards non-invasive blood glucose measurement using machine learning: An all-purpose PPG system design,” Biomedical Signal Processing and Control, vol. 68, p. 102706, Jul. 2021.

[6] A. Prabha, J. Yadav, A. Rani, and V. Singh, “Intelligent estimation of blood glucose level using wristband PPG signal and physiological parameters,” Biomedical Signal Processing and Control, vol. 78, p. 103876, Sep. 2022.

[7] C.-T. Yen, U.-H. Chen, G. Wang, and Z. Chen, “Non-Invasive Blood Glucose Estimation System Based on a Neural Network with Dual-Wavelength Photoplethysmography and Bioelectrical Impedance Measuring,” Sensors, vol. 22, no. 12, pp. 4452–4452, Jun. 2022.

[8] S. M. Taslim Uddin Raju and M. M. A. Hashem, "DNN Based Blood Glucose Level Estimation Using PPG Characteristic Features of Smartphone Videos," 2022 25th International Conference on Computer and Information Technology (ICCIT), Cox's Bazar, Bangladesh, 2022, pp. 13-18.

[9] S. Alghlayini, A. Hosni and M. Atef, "Photoplethysmography Based Blood Glucose Estimation Using Convolutional Neural Networks," 2023 Advances in Science and Engineering Technology International Conferences (ASET), Dubai, United Arab Emirates, 2023.

[10] S. Hossain, B. Debnath, S. Biswas, M. J. Al-Hossain, A. Anika and S. K. Zaman Navid, "Estimation of Blood Glucose from PPG Signal Using Convolutional Neural Network," 2019 IEEE International Conference on Biomedical Engineering, Computer and Information Technology for Health (BECITHCON), Dhaka, Bangladesh, 2019, pp. 53-58

[11] T. T. Islam, M. S. Ahmed, M. Hassanuzzaman, S. A. Bin Amir, and T. Rahman, “Blood Glucose Level Regression for Smartphone PPG Signals Using Machine Learning,” Applied Sciences, vol. 11, no. 2, p. 618, Jan. 2021.

[12] C. R. Monnard and E. K. Grasser, “Perspective: Cardiovascular Responses to Sugar-Sweetened Beverages in Humans: A Narrative Review with Potential Hemodynamic Mechanisms,” Advances in Nutrition, vol. 9, no. 2, pp. 70–77, Mar. 2018.

[13] G. Zhang et al., “A Non-invasive Blood Glucose Monitoring System Based on Smartphone PPG Signal Processing and Machine Learning,” IEEE Transactions on Industrial Informatics, pp. 1–1, 2020.

[14] J. Park, H. S. Seok, S.-S. Kim, and H. Shin, “Photoplethysmogram Analysis and Applications: An Integrative Review,” Frontiers in Physiology, vol. 12, Mar. 2022.

[15] G. Tusman et al., “Photoplethysmographic characterization of vascular tone mediated changes in arterial pressure: an observational study,” Journal of Clinical Monitoring and Computing, vol. 33, no. 5, pp. 815–824, Oct. 2019.

[16] A. A. Awad et al., “The relationship between the photoplethysmographic waveform and systemic vascular resistance,” Journal of Clinical Monitoring and Computing, vol. 21, no. 6, pp. 365–372, Oct. 2007.

[17] E. Susana, K. Ramli, H. Murfi, and N. H. Apriantoro, “Non-Invasive Classification of Blood Glucose Level for Early Detection Diabetes Based on Photoplethysmography Signal,” Information, vol. 13, no. 2, p. 59, Jan. 2022.

[18] E. Pintelas, I. E. Livieris, and P. E. Pintelas, “A Convolutional Autoencoder Topology for Classification in High-Dimensional Noisy Image Datasets,” Sensors, vol. 21, no. 22, p. 7731, Nov. 2021.

[19] “Nano 33 BLE Sense | Arduino Documentation,” docs.arduino.cc. https://docs.arduino.cc/hardware/nano-33-ble-sense.

[20] R. David et al., “TensorFlow Lite Micro: Embedded machine learning for TinyML systems,” in Proc. Mach. Learn. Syst., vol. 3, 2021, pp. 1–12.

[21] P.-L. Lee, K.-W. Wang, and C.-Y. Hsiao, “A Noninvasive Blood Glucose Estimation System Using Dual-Channel PPGs and Pulse-Arrival Velocity,” IEEE Sensors Journal, vol. 23, no. 19, pp. 23570–23582, Oct. 2023.

[22] J. Li et al., “Noninvasive Blood Glucose Monitoring Using Spatiotemporal ECG and PPG Feature Fusion and Weight-Based Choquet Integral Multimodel Approach,” IEEE transactions on neural networks and learning systems, pp. 1–15, Jan. 2023.